Investigation on mechanical properties, durability and micro-structural development of steel slag blended cements

Tongsheng Zhang · Qijun Yu · Jiangxiong Wei · Jianxin Li

Abstract To improve the properties of steel slag blended cements, a chemical activator was added into blended cements, the mechanical properties and durability of steel slag blended cements were investigated. The results show that steel slag in blended cement pastes presents low hydraulic activity and makes practically no contribution to strength development. After the addition of chemical activator, the mechanical properties and durability of ternary blended cements are increased significantly. The hydration process and micro-structural development of blended cement was investigated by isothermal calorimeter and scanning electric microscope, respectively. Steel slag started hydration in the first 3 days in the presence of chemical activator, steel slag and granulate blast furnace slag reacted with $Ca(OH)_2$ to form a dense microstructure as curing proceeded. Therefore, both early and late compressive strengths of steel slag blended cement with 35% cement clinker and 30% steel slag can be comparable with those of Portland cement.

Keywords Steel slag · Blended cement · Mechanical properties · Durability · Microstructure

Introduction

Steel slag, a by-product of steel making industry, is produced during the separation of molten steel from impurities in steel-making furnaces, and the amount of steel slag is about 12–20% by mass of produced steel. China produces about 85 million tons of steel slag annually, and the total amount of deposited steel slag is about 400 million tons. Chemical and mineral compositions of steel slag obtained from converters are similar to those of cement clinker [1], therefore, steel slag is a cementitious material in potential, and can be used as supplementary cementitious materials (SCMs) to produce steel slag blended cements, which has been noted for both environmental and economical advantages [2–4]. Owing to difficulties in cooling the steel slag very quickly, the cementitious minerals in steel slag, such as C_3S and C_2S, are relatively inert to react with water compared with those of cement clinker [5], which leads to relatively low early strengths of blended cements containing steel slag. Meanwhile the substitution level of steel slag in blended cement is limited to about 15% by mass in industrial practices [6]. Thus methods on how to improve the properties of steel slag blended cements are being highlight.

Chemical activators for SCMs are cement clinker, gypsums, alkalis, sulfates, and other similarities [7, 8]. But the results are not satisfied because of large dosage of activators or undesirable activating effects. It is possible that silicates can be activated by a similar dissolution and geo-polymerization process when contacted with the mixture of alkalis and sulfates. With such a possibility, a composite activator was added into steel slag blended cements, the mechanical properties, durability and micro-structural development of steel slag blended cements with or without activator were closely investigated.

Raw materials

Portland cement clinker used in the experiment was provided by Zhujiang cement plant. Steel slag and granulate

T. Zhang · Q. Yu · J. Wei (✉) · J. Li
Key Laboratory of Specially Functional Materials
of the Ministry of Education, South China University
of Technology, 510640 Guangzhou, China
e-mail: jxwei@scut.edu.cn

blast furnace slag (BFS) were obtained from Jinan iron and steel group. The steel slag used was collected from converters and has been heaped up in the out-door conditions for several years before milling. A low calcium fly ash (Class F fly ash according to ASTM C 618 [9]), having low carbon content and high Blaine fineness (463 m^2/kg), was collected from the last hopper of Zhujiang powder plant. The chemical compositions of raw materials measured by X-ray fluorescence spectroscopy (XRF) are summarized in Table 1, which present a higher amount of Fe_2O_3 and MgO and a lower content of SiO_2 and CaO in steel slag when compared with Portland cement clinker.

The minerals of the steel slag determined by X-ray diffraction (XRD, 40 kV, 15 mA, $CuK_{\alpha 1}$, 0.05°/2θ step size, and 3 s/step) are mainly C_3S, C_2S (mainly γ-C_2S and minor β-C_2S), $2CaO \cdot (Al,Fe)_2O_3$, Ca_2Fe, $CaCO_3$ and RO phase (a solid solution between MgO (periclase), MnO and FeO (wustite)) as shown in Fig. 1, among which only C_3S and β-C_2S can exhibit cementitious property under normal hydration condition. It can be concluded that the cementitious properties of the steel slag is very weak due to low C_3S and β-C_2S content. Although small amount of free CaO always presents in the steel slag, it could not be clearly identified by XRD here. This may be due to the content of free CaO, which is not sensitive to XRD [10]. However, $CaCO_3$ was identified in the steel slag due to carbonation of $Ca(OH)_2$ during out-door treatments.

Preparation of blended cements

In previous experiments [11], the optimal mixture proportions of clinker, steel slag, BFS, and fly ash in steel slag blended cement were determined. Clinker-steel slag (PS) cement, clinker-BFS (PB) cement, clinker-fly ash (PF) cement, and ASTM type I Portland cement (PI) were also prepared as references. Chemical activator used in present study is a mixture of water–glass ($Na_2O/SiO_2 = 1.3$), CaO and $KAl(SO_4)_2$ at the mass ratio of 6:2:1. As usual, gypsum dihydrate was used to adjust the setting time of the blended cements. Mixture proportions of blended cements are listed in
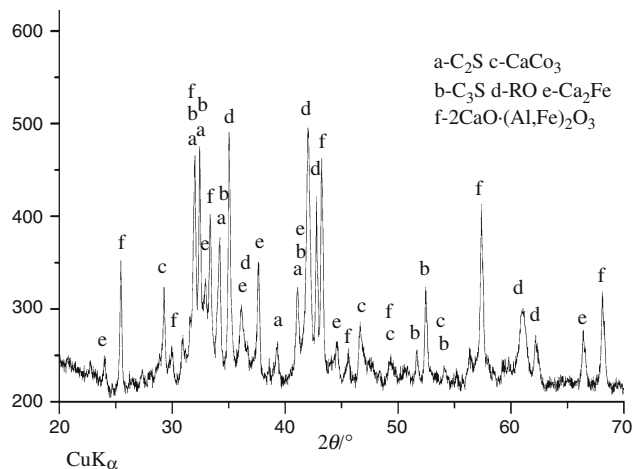

Fig. 1 X-ray diffraction pattern of steel slag used in the experiment

Table 2. Raw materials were weighted and ground in a laboratory ball mill, the specific surface areas of these cements were controlled to be in the range of 350–360 m^2/kg.

Fundamental properties of steel slag blended cements

Water requirement, setting time, and soundness

Water requirements for normal consistency, setting times, boiling soundness, and autoclaved soundness of steel slag blended cements were determined according to EN 196-3 [12] and ASTM C151-09 [13]. Table 3 shows that PS cement paste has the lowest water requirement for normal consistency and the longest setting time, more important, both boiling soundness and autoclaved soundness are failed. SSBC cement paste also shows low water requirement and decreased setting time, while autoclaved soundness can not meet the requirement of ASTM C151-09 (0.5% expansion ratio for blended cement). The setting time of steel slag blended cement paste with chemical activator (SSBCJ) reduces sharply; both boiling soundness and autoclaved soundness of SSBCJ paste can meet the requirements of EN 196-3 and ASTM C151-09.

Table 1 Chemical compositions of Portland cement clinker, BFS, low calcium fly ash and steel slag used in the experiment

Material	Chemical composition/%									
	SiO_2	Al_2O_3	Fe_2O_3	CaO	MgO	K_2O	Na_2O	SO_3	TiO_2	LOI
Portland cement clinker	21.86	4.45	2.35	63.51	1.67	0.55	0.26	2.91	0.11	1.89
Steel slag	15.84	3.59	21.14	41.14	7.33	0.05	0.05	0.61	0.81	7.91
BFS	35.22	12.15	0.25	37.08	11.25	0.49	0.25	1.19	0.73	−0.36
Low calcium fly ash	50.28	29.16	5.37	7.51	1.24	1.20	0.67	0.30	0.69	0.96

LOI loss on ignition

Table 2 Mixture proportions of steel slag blended cements (by mass)

Cement Id.	Mixture proportion/%					
	Clinker	Steel slag	BFS	Fly ash	Gypsum	Activator
PI	95	–	–	–	5	0
PS	35	60	–	–	5	0
PB	35	–	60	–	5	0
PF	35	–	–	60	5	0
SSBC	35	30	25	5	5	0
SSBCJ	35	30	22	5	5	3

Mechanical properties

Mortar prisms of $40 \times 40 \times 160$ mm were prepared at water: cement: standard sand [14] mass ratio of 0.5:1:3. After curing at 20 ± 1 °C and 90% relative humidity (RH) for 24 h, the specimens were demoulded and cured in lime-saturated water at 20 ± 1 °C, followed by strength tests according to EN 196-1 [15].

Figure 2 shows that both 3 and 28 days compressive strengths of blended cements with equal clinker content mainly depend on the types of SCMs incorporated. PS and PF cements present relatively lower 3 days compressive strength due to low activity of steel slag and fly ash. While the compressive strengths of SSBC are approximately equal to that of PB cement. That is to say, the co-contribution of steel slag, fly ash and BFS to the strengths of SSBC is much higher than the summary of their single contributions. Both 3 and 28 days compressive strengths of SSBCJ increase remarkably (especially for 3 days compressive strength), and can be comparable with those of the Portland cement (PI).

Durability of steel slag blended cement mortars

Resistance against sulfate attack

Mortar prisms of selected blended cements after 28 days of curing in lime-saturated water were placed in 5% Na_2SO_4 solutions and lime-saturated water, respectively. After 90 and 180 days of exposing in aggressive medium, the compressive strength of mortars was tested as specified in EN 196-1. Figure 3 indicates that the compressive strength of PS blended cement exposed in 5% Na_2SO_4 solutions is declined significantly, especially for 180 days exposing. However, the compressive strengths of SSBC and SSBCJ blended cements exposed in aggressive medium are increased slightly or remain unchanged, indicating that "pore size reinforcement" caused by pozzolanic reaction leads to a better resistance against sulfate attack [16].

Drying shrinkage

Mortar prisms of $25 \times 25 \times 280$ mm were prepared at cement to sand ratio of 0.5, and the fluidity of mortars was controlled in the range of 130–140 mm by adjusting water addition. After being cured at 20 ± 1 °C and 90% RH for 24 h, the specimens were demoulded and subsequently cured in lime-saturated water at 20 ± 1 °C for 2 days. Initial lengths of the specimens were measured immediately after curing, then the specimens were exposed to a 20 ± 1 °C and 50% RH environmental chamber and the length changes were measured at different ages [17]. Figure 4 shows that most of drying shrinkage of cement mortar takes place in the first 42 days. PS cement shows very high drying shrinkage ratio. In contrast, SSBC cement presents relatively lower drying shrinkage ratio, and the

Table 3 Water requirement for normal consistency and soundness of steel slag blended cements

| Cement Id.	Water requirement for normal consistency	Setting time/min		Boiling soundness		Autoclaved soundness	
		Initial	Final	Chatelier's value/mm	Passed or failed	Expansion ratio/%	Passed or failed
PI	0.243	109	174	2.5	Passed	0.25	Failed
PS	0.237	292	374	6.9	Failed	1.33	Failed
PB	0.249	184	282	2.5	Passed	0.22	Failed
PF	0.252	205	290	2.0	Passed	0.27	Passed
SSBC	0.239	169	234	3.8	Passed	0.63	Passed
SSBCJ	0.252	123	196	3.1	Passed	0.32	Passed

a

b
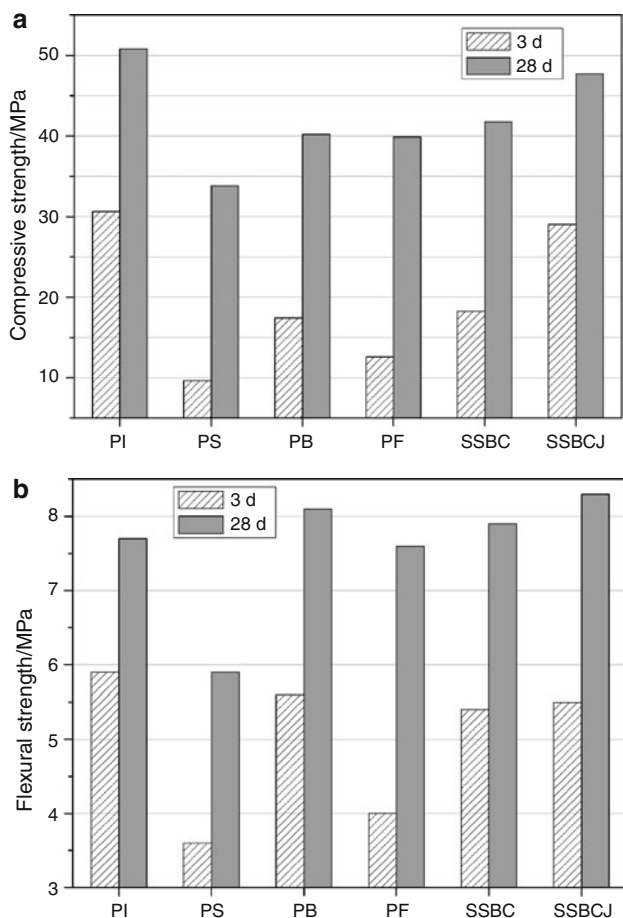
Fig. 2 Compressive and flexural strengths of steel slag blended cements **a** Compressive strength, **b** Flexural strength

drying shrinkage ratio of SSBCJ cement is even slightly lower than that of Portland cement.

Heat evolution of steel slag blended cement pastes

The heat evolution of cement pastes made at water to cementitious material mass ratio of 0.5 were followed for 72 h at 25 °C using a TAM-Air isothermal calorimeter according to ASTM C 1702-09 [18].

Figure 5 shows that Portland cement (PI) presents the highest rate of heat evolution and cumulative heat of hydration. In contrast, PS cement shows the lowest rate of heat evolution and cumulative heat of hydration due to low hydraulic activity of steel slag. SSBC cement gives a relatively higher rate of heat evolution than PS cement. After the addition of chemical activator, both rate of heat evolution and cumulative heat of hydration of SSBCJ cement are increased significantly. The 3 days cumulative heat of hydration of SSBCJ tested was about 80% of that of Portland cement. Clearly, the hydration of SCMs in SSBCJ
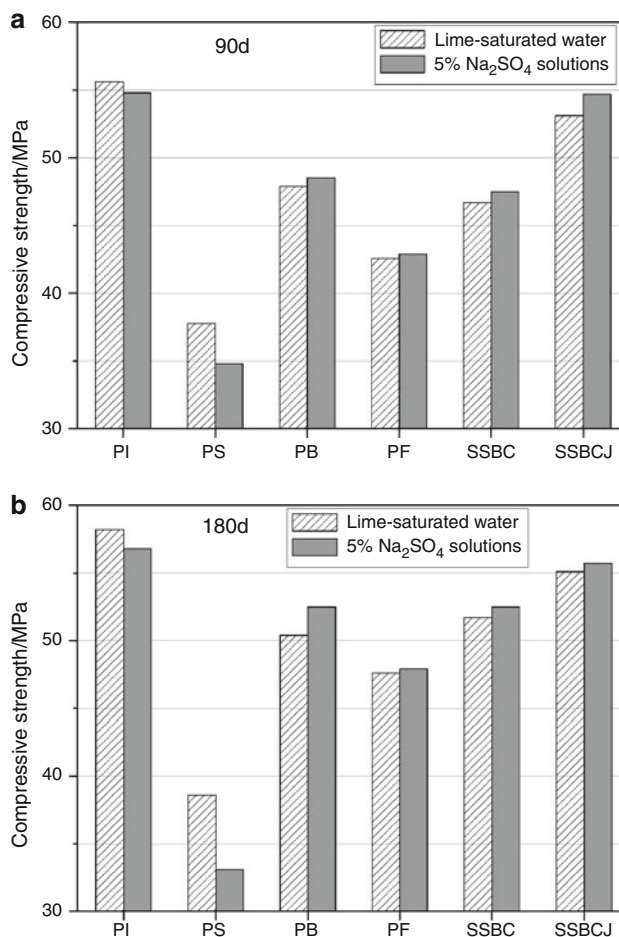
a

b

Fig. 3 Compressive and flexural strengths of steel slag blended cement mortars cured in 5% Na_2SO_4 solutions **a** Cement mortars cured for 90 days, **b** Cement mortars cured for 180 days
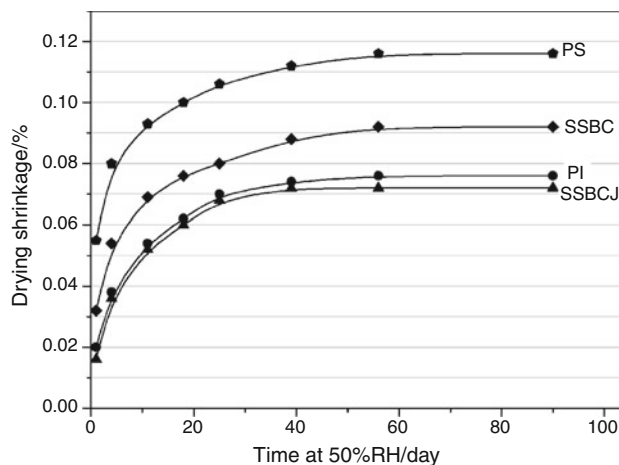

Fig. 4 Drying shrinkage of steel slag blended cement mortars at 50% RH and 20 ± 1 °C

cement is much more significance than that in PS or SSBC cements. Similar phenomenon was also found for Portland zeolite cement [19–21].

Micro-structural development of steel slag blended cement pastes

Cement pastes made at normal consistency (water requirement for normal consistency was given in Water requirement, setting time, and soundness) were cast into plastic bags and sealed before placed in a 20 ± 1 °C water bath. Small pieces taken from different parts of the hardened pastes were put into ethyl alcohol to stop hydration after 1, 3, and 28 days, then vacuum-oven-dried at 40 °C for at least 48 h. Hydration products of blended cement were characterized by XRD, microstructures of hardened cement pastes were observed using a scanning electric microscope (SEM, Nano 430, 10 kV) and their pore size distributions were measured by mercury intrusion porosimetry (MIP, Poremaster-60, contact angle 140.7°) with an operating pressure up to about 500 MPa.

Hydration products of hardened cement pastes

X-ray diffraction patterns of hardened cement pastes are shown in Fig. 6. It can be found that the types of hydration

Fig. 5 Heat evolution curves of Portland cement and steel slag blended cements **a** Rate of heat evolution, **b** Cumulative heat of hydration

products of the steel slag blended cements prepared are the same as those of Portland cement. Comparing with the XRD pattern of Portland cement, the diffraction peaks corresponding to C–S–H gel and AFt crystals in SSBC paste are relatively low, and a much higher diffraction peak of C_2S is observed, indicating large amount of C_2S in steel slag remains un-hydrated after 28 days curing. In contrast, the diffraction peak of $Ca(OH)_2$ crystal is scarcely found in SSBCJ paste, and the intensity of the diffraction peaks of AFt and C–S–H gel are much higher than that of SSBC paste. It is suggested that the hydration products of steel slag blended cements with chemical activator (containing sulfate) are mainly C–S–H gel and AFt.

Microstructures of hardened cement pastes

SEM images of hardened cement pastes are depicted in Fig. 7. Figure 7a demonstrates a loosen microstructures, consisting of small amount of hydration products (mainly C–S–H gel and $Ca(OH)_2$) and large amount of large-sized pores, in PS cement paste cured for 3 days. For PS cement paste cured for 28 days (Fig. 7b, c), large amount of $Ca(OH)_2$ and small amount of hydration products are found, and there is an obvious gap between un-hydrated steel slag particles and hydration products. It can be concluded that steel slag in PS cement presents very low hydraulic activity and makes practically no contribution to the strength development of blended cement.

In comparison with PS cement paste, smaller amount of pores is observed in SSBC cement paste, the microstructures of SSBC cement paste cured for both 3 and 28 days appears denser as shown in Fig. 7d–f. Steel slag particles had surface hydrated after 28 days curing (Fig. 7e, f), meanwhile the gap between steel slag particles and hydration products became vague.
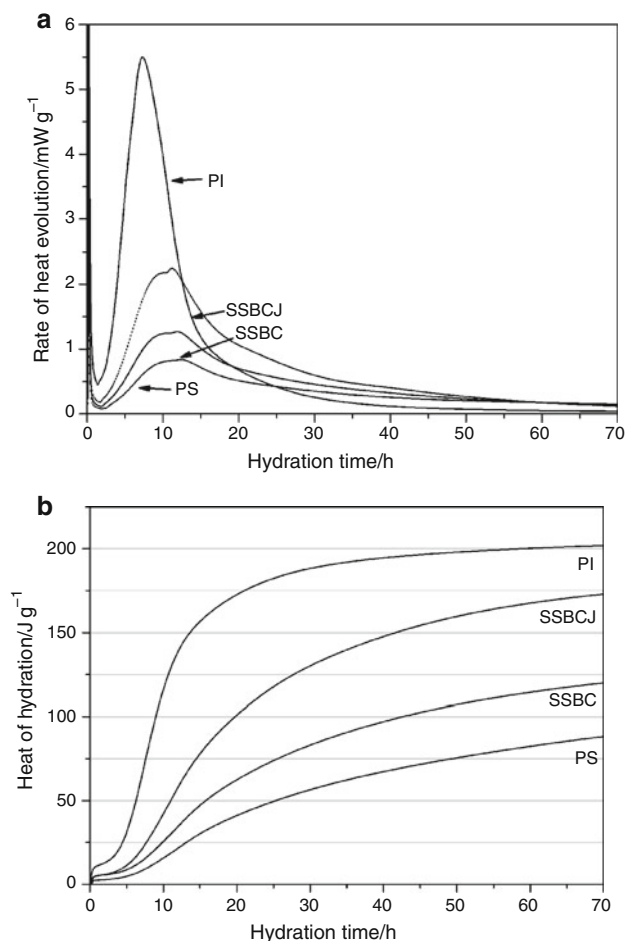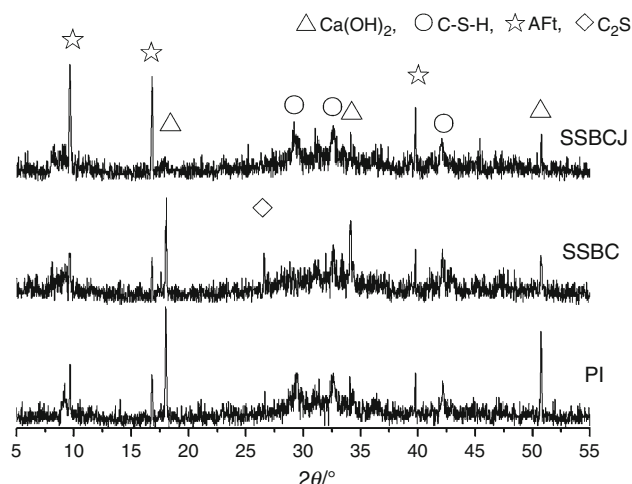
Fig. 6 X-ray diffraction patterns of hardened steel slag blended cement pastes cured 28 days

Fig. 7 SEM images of hardened cement pastes **a** PS cement paste cured for 3 days, **b** and **c** PS cement paste cured for 28 days, **d** SSBC cement paste cured for 3 days, **e** and **f** SSBC cement paste cured for 28 days, **g** SSBCJ cement paste cured for 3 days, **h** and **i** SSBCJ cement paste cured for 28 days
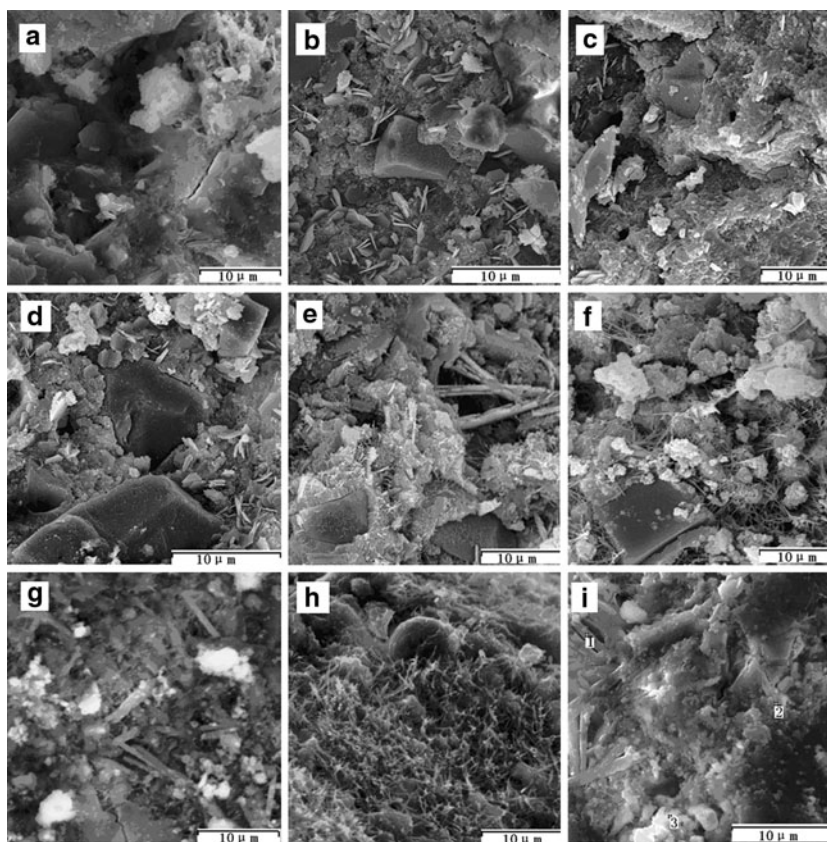
Table 4 Porosity and pore size distribution of hardened cement pastes cured for 28 days

Cement Id.	Porosity/%	Model pore diameter/nm	Pore size distribution/%				
			<10 nm	10–50 nm	50–100 nm	100–1000 nm	>1000 nm
PS	31.5	218.0	1.5	8.7	24.1	43.7	22.0
SSBC	26.7	106.7	4.7	15.9	45.7	22.6	11.1
SSBCJ	21.8	76.3	8.7	20.5	50.6	12.8	7.4

Figure 7g demonstrates that SSBCJ cement paste had a dense network structure, consisting of well-combined hydration products, such as C–S–H gel and bar-like AFt. Furthermore, no obvious gap between steel slag particles and hydration products is observed, indicating steel slag started hydration in the first 3 days. After 28 days curing (Fig. 7h, i), the mount of hydration products increases steadily, and $Ca(OH)_2$ is scarcely found. The results prove that after the addition of the composite activator, $Ca(OH)_2$ reacts with SCMs to form more C–S–H gel and AFt, which intertwining with each other, filling the pores, and forming a denser microstructures [22].

Pore size distribution of hardened cement pastes

Porosity and pore size distribution of hardened blended cement pastes are depicted in Table 4. It is significant that

PS cement paste has the highest porosity and large amount of pores beyond 100 nm. In contrast, SSBC cement paste has lower porosity and small amount of large-sized pores. Furthermore, SSBCJ cement paste has the lowest porosity and smaller amount of large-sized pores. The results proved that after addition of activator, a large amount of new generated hydration products filling large-sized pores into smaller ones [23], therefore the microstructures of steel slag blended cement pastes become denser due to more significant pozzolanic reaction or hydration of SCMs. The results consist with the above conclusion drawn from SEM observation.

Conclusions

Main conclusions drawn form the experimental study can be summarized as follows:

(1) Steel slag in blended cement pastes presents low hydraulic activity and makes practically no contribution to strength development.

(2) The co-contribution of steel slag, fly ash and BFS to the strengths of steel slag blended cements is much higher than the summary of their single contributions.

(3) After the addition of chemical activator, both early and late compressive strengths of steel slag blended cement with 35% cement clinker and 30% steel slag can be comparable with those of Portland cement. The blended cement also presents good resistance against sulfate attack and low drying shrinkage.

(4) Steel slag started hydration in the first 3 days in the presence of chemical activator, $Ca(OH)_2$ reacts with SCMs to form more C–S–H gel and AFt, which intertwining with each other, filling the pores, and forming a denser microstructures.

References

1. Xu Y, Lu W, Wang X. Research and development in activation of steel slag activity. J Shanghai Univ. 2004;10:91–6.

2. Zhu G, Sun S, Wu G. The characters and estimate method of cementitious properties of steel slag. The fourth Chinese cement academic conference anthology. Beijing: Chinese Building Materials Publisher; 1992. p. 759–69 (in Chinese).

3. Zhang TS, Yu QJ, Wei JX, Gao P, et al. Study on optimization of hydration process of blended cement. J Therm Anal Calorim. 2011. doi:10.1007/s10973-011-1531-8.

4. Pacewska B, Blonkowski G, Wilińska I. Investigation of the influence of different fly ashes on cement hydration. J Therm Anal Calorim. 2006;86:179–86.

5. Shi C, Qian J. High performance cementing materials from industrial slags. Resour Conserv Recycl. 2000;29:195–207.

6. Qian G. Actions of alkali contents and pH in the solution on cement strength of steel-slag with lower alkali basicity and a few of clinker. J Southwest Institute Technol. 1997;12:17–20.

7. Hu S, Jiang C, Wei J. Research on hydration of steel slag cement activated with water-glass. J Wuhan Univ Technol. 2001;16:37–9.

8. Hu S, He Y, Lu L. Effect of fine steel slag power on the early hydration process of Portland cement. J Wuhan Univ Technol. 2006;21:147–9.

9. ASTM C 618-03. Standard specification for fly ash and raw or calcined natural pozzolan for use as a mineral admixture in Portland cement concrete. American Society for Testing and Materials; 2006.

10. Shi Cj. Characteristics and cementitious properties of ladle slag fines from steel production. Cem Concr Res. 2002;32:459–62.

11. Zhang T, Liu F, Liu S. Factors influencing the properties of a steel slag composite cement. Adv Cem Res. 2008;20:145–50.

12. EN 196-3. Methods of testing cement: determination of water requirement for normal consistency. European Standards; 2005.

13. ASTM C151-09. Test method for autoclave expansion of hydraulic cement. American Society for Testing and Materials; 2009.

14. GB 178-1997. ISO standard sand for determination of cement mortar strength (ISO 769). Chinese Standards; 1997.

15. EN 196-1. Methods of testing cement: determination of strength. European Standards; 2005.

16. Janotka I, Krajči L. Sulphate resistance and passivation ability of the mortar made from pozzolan cement with zeolite. J Therm Anal Calorim. 2008;94:7–14.

17. ASTM C596-96. Standard test method for drying shrinkage of mortar containing hydraulic cement. American Society for Testing and Materials; 2000.

18. ASTM C 1702-09A. Standard test method for measurement of heat of hydration of hydraulic cementitious materials using isothermal conduction calorimetry. American Society for Testing and Materials; 2009.

19. Snellings R, Mertens G, Elsen J. Calorimetric evolution of the early pozzolanic reaction of natural zeolites. J Therm Anal Calorim. 2010;101:97–105.

20. Kontori E, Perraki T, Tsivilis S, Kakali G. Zeolite blended cements: evaluation of their hydration rate by means of thermal analysis. J Therm Anal Calorim. 2009;96:993–8.

21. Gruyaert E, Robeyst N, De Belie N. Study of the hydration of Portland cement blended with blast-furnace slag by calorimetry and thermogravimetry. J Therm Anal Calorim. 2010;102:941–51.

22. Chaipanich A, Nochaiya T. Thermal analysis and microstructure of Portland cement-fly ash-silica fume pastes. J Therm Anal Calorim. 2010;99:487–93.

23. Krajči L, Moujmdar SC, Kuliffayová M, Janotka I. Microstructure of Portland cement mortar amended by burnt kaolin sand. J Therm Anal Calorim. 2010;100:779–87.